Published in final edited form as:

AJNR Am J Neuroradiol. 2015 December ; 36(12): 2360–2366. doi:10.3174/ajnr.A4454.

Optimal prediction of carotid intraplaque hemorrhage using clinical and lumen imaging markers

Michael S. McLaughlin, MD[1], **Peter J. Hinckley, BS**[1], **Scott M. Treiman**[1], **Seong-Eun Kim, PhD**[1], **Gregory J. Stoddard, MBA, MPH, PhD**[2], **Dennis L. Parker, PhD**[1], **Gerald S. Treiman, MD**[1,3,4], and **J. Scott McNally, MD, PhD**[1]

[1]Utah Center for Advanced Imaging Research, Department of Radiology, University of Utah

[2]Study Design and Biostatistics Center, Department of Orthopedics, University of Utah

[3]Department of Surgery, VA Salt Lake City Health Care System

[4]Department of Surgery, University of Utah

Abstract

Purpose—MRI detects intraplaque hemorrhage (IPH) with high accuracy using the magnetization-prepared rapid acquisition gradient echo (MPRAGE) sequence. Still, MRI is not readily available for all patients, and many receive CTA instead. Our goal was to determine essential clinical and lumen imaging predictors of IPH as indicators of its presence and clues to its pathogenesis.

Methods—In this retrospective cross sectional study, patients undergoing stroke workup with MRI/MRA underwent carotid IPH imaging. A total of 726 carotid plaques were analyzed, excluding vessels with non-carotid stroke sources (420), occlusions (7), or near-occlusions (3). Potential carotid imaging predictors of IPH included percent diameter and mm stenosis, plaque thickness, ulceration, and intraluminal thrombus. Clinical predictors were recorded and a multivariable logistic regression model was fitted. Backward-elimination was used to determine essential IPH predictors with a threshold two-sided p<.10. Receiver operating characteristic (ROC) analysis was also performed.

Results—Predictors of carotid IPH included plaque thickness (odds ratio, OR=2.20, p<.001), mm stenosis (OR=0.46, p<.001), ulceration (OR=4.25, p=.020), age (OR=1.11, p=.001) and male sex (OR=3.23, p=.077). The final model discriminatory value was excellent (area under the curve, AUC=0.932). This was significantly higher than models using only plaque thickness (AUC=0.881), mm stenosis (AUC=0.830) or ulceration (AUC=0.715) p<.001.

Conclusions—Optimal discrimination of carotid IPH requires information on plaque thickness, mm stenosis, ulceration, age and male sex. These factors predict IPH with high discriminatory power, and may provide clues to the pathogenesis of IPH. This model could be used to predict the presence of IPH when MRI is contraindicated.

Corresponding author: J. Scott McNally, University of Utah, Department of Radiology, 30 N 1900 East, Salt Lake City, UT 84132, Fax: 801-581-2424, Office: 801-585-1003, scott.mcnally@hsc.utah.edu.

Introduction

For over 20 years, stenosis has been the primary predictor of stroke risk from carotid disease based on landmark studies including the North American Symptomatic Carotid Endarterectomy Trial (NASCET), Asymptomatic Carotid Atherosclerosis Study (ACAS) and European Carotid Surgery Trial (ECST) trials.[1–3] Over the last 10 years, advances have been made in MRI-detection of plaque components, most notably with carotid intraplaque hemorrhage (IPH). High MRI signal within the carotid wall was first shown to detect complex atheromas by Moody and colleagues.[4] Since that time, carotid IPH has been detectable with high accuracy using heavily T1-weighted sequences such as magnetization-prepared rapid acquisition gradient echo (MPRAGE).[5] MRI-detected carotid IPH is an essential indicator of stroke risk, and is independent of stenosis.[6–9] However, MRI in general and the MPRAGE sequence specifically may not be available in all clinical settings.

While most reports have correlated IPH with other markers of plaque vulnerability, none have generated a predictive model of IPH based on all available clinical and imaging markers. Many researchers have demonstrated that IPH increases in likelihood with increasing carotid stenosis.[10] Others have shown that IPH positively correlates not only with stenosis, but also with plaque volume or thickness.[11] Recently, CTA-detected ulceration was found to act as a surrogate marker for IPH.[12] These data suggest that IPH can be predicted with some degree of accuracy based on lumen imaging findings. In addition, IPH has been found at higher prevalence in males and in higher age groups.[13] With these findings in mind, the goal of this study was to determine a predictive model of IPH using available imaging and clinical markers.

We began with the hypothesis that lumen imaging and clinical factors could be used to predict the presence of IPH. By doing so, this may provide clues to the pathogenesis of IPH. Another potential benefit would be to patients in which MRI is contraindicated. To detect IPH, we used an MPRAGE sequence included as part of a clinical protocol beginning in November 2009. Data was gathered prospectively and analyzed in a retrospective cross sectional study. We included all patients imaged with carotid MRA using the MPRAGE sequence over the course of 4.5 years. A multivariable logistic regression model was fitted to determine essential imaging and clinical markers of IPH. This cohort of patients was used previously to determine predictors of carotid-source stroke, which were found to include intraluminal thrombus, intraplaque hemorrhage, plaque thickness and current smoking.[8]

Methods

Clinical study design

IRB approval was obtained for this cross sectional study on patients undergoing stroke evaluation with brain MRI/carotid MRA from November 2009–January 2014. The carotid MPRAGE sequence was added to the clinical MRA imaging protocol in November 2009. Patients presenting for stroke workup were scanned within 1 week of symptom onset. From November 2009 to January 2014, 578 patients underwent brain MRI/carotid MRA for acute stroke evaluation with the additional MPRAGE sequence. This resulted in 1156 carotid artery-ipsilateral brain image pairs.

Exclusions were determined after reviewing electronic medical records for non-carotid plaque stroke sources – those outside of 2 cm above and below the carotid bifurcation. There were 420 carotid-brain pairs excluded. These included craniocervical dissections (118), atrial fibrillation (94), intracardiac/extracardiac shunt (86), cardiac thrombus (26), recent aortic or mitral valve replacement (16), vasculitis (14), global hypoxic/ischemic injury (10), recent cardiac or neurovascular catheterization (10), recent cardiovascular surgery (8), dural venous sinus thrombosis (8), fibromuscular dysplasia or lupus vasculopathy (8), proximal common carotid stenosis >50% (6), rheumatic heart disease (4), brain neoplasm (4), endocarditis (2), idiopathic hypertrophic subaortic stenosis (2), aortic graft complication (2), and distal vessel atherosclerosis (2). We also excluded occluded carotid arteries (7) and extremely high grade lesions (3). 726 carotid plaques were used in the final analysis. Although a few scans exhibited mild motion artifacts primarily from swallowing, these artifacts were not sufficient to exclude any carotid arteries from interpretation.

MRI/MRA clinical protocol

Images were obtained on Siemens 3T and 1.5T MRI scanners with standard head/neck coils. The standard clinical MRI/MRA protocol for these patients included brain MRI (axial DWI, axial T2-weighted, axial FLAIR and sagittal T1-weighted images), brain MRA (3D axial TOF) and neck MRA (2D axial TOF, coronal precontrast T1-weighted, coronal postcontrast arterial and venous phase images). Coronal postcontrast MRA neck images were obtained from the aortic arch through the circle of Willis. Total scan time was approximately 45 minutes, of which the MPRAGE sequence required approximately 5 minutes. In cases when renal insufficiency precluded intravenous contrast (GFR < 30 ml/min/1.73m^2), postcontrast MRA images were replaced with 3D noncontrast TOF with 1 mm slice thickness combined with duplex ultrasound.

Carotid MPRAGE sequence

MPRAGE parameters were first optimized at 3T and were as follows: 3D, TR/TE/ TI = 6.39/2.37/370 ms, flip angle = 15 degrees, FOV = 130 × 130 × 48 mm^3, matrix = 256 × 256 × 48, voxel = 0.5 × 0.5 × 1.0 mm^3, fat saturation, time ~ 5 minutes. The TI was initially optimized for 3T and transferred to 1.5T. An initial TI of approximately 500 ms was chosen based on prior computer simulations at 3T and was adjusted down to a TI of 370 ms to maximize contrast between hemorrhage and inflowing blood in human volunteers as described previously.[14, 15] Images were obtained from 20 mm below to 20 mm above the carotid bifurcation at 1.0 mm slice thickness. In order to produce 3D images, a secondary phase encoding gradient was used in the slice select direction and measurements for all slice selection phase encodings were performed with rapid acquisition in each segment.

Carotid lumen imaging markers

All carotid imaging markers were determined by consensus review of 2 reviewers (M.S.M. and J.S.M.), both blinded to findings on brain MRI and clinical covariates. In addition, IPH was determined independently of other carotid imaging markers of stroke risk. Lumen markers included percent diameter stenosis, mm stenosis, maximum plaque thickness, ulceration and intraluminal thrombus.

Percent diameter stenosis was determined using NASCET criteria on contrast MRA. Briefly, the diameter (b) at the level of maximal stenosis and diameter (a) of the internal carotid artery (ICA) distal to the stenosis were used to calculate percent diameter stenosis using the formula [(a-b)/a]*100%. Carotid stenosis was measured at the narrowest segment of the carotid plaque (b) on the axial images, perpendicular to the long axis of the vessel on multiplanar reformats using a sub-mm measurement tool (Figure 1A). The distal ICA diameter (a) was measured beyond the bulb where the walls are parallel and no longer tapering per NASCET criteria.[16–18] We performed the multivariable regression analysis using both the NASCET measurement of percent diameter stenosis [(a−b)/a]*100% and a mm stenosis (b) measurement, adapted from the mm stenosis method first described on CTA.[19] To identify near occlusions, an ICA was excluded from percent stenosis calculation if it met the following criteria: visible bulb stenosis, distal ICA diameter ≤3 mm, and distal ICA/distal ECA ratio of ≤1.25. These criteria were further adapted from those used by Bartlett et al to recognize subtle near-occlusions on CTA, and originally adapted from standard conventional angiography.[18, 19]

The presence of ulceration was determined on contrast MRA images using a size threshold of 2 mm as previously described with CTA (Figure 1B).[12] Intraluminal thrombus was defined by an intraluminal filling defect on MRA axial reformats, previously described on CTA (Figure 1C).[20] In arteries from patients with renal failure (GFR < 30 ml/min/1.73m^2, 68/726 or 9.4% of carotid-brain image pairs), the above imaging markers were determined from 3D noncontrast TOF with 1 mm slice thickness combined with duplex ultrasound. Maximum plaque thickness was measured in the transverse plane on MPRAGE images (Figure 1D). IPH was defined quantitatively as MPRAGE-positive plaque, with at least 1 voxel demonstrating at least 2-fold higher signal intensity relative to adjacent sternocleidomastoid muscle as previously described (Figure 1D right carotid is MPRAGE positive, image left).[6]

Statistical analysis

A mixed effects multivariable logistic regression model was used. This model accounted for 2 vessels per patient. The multivariable logistic regression model was fitted for the outcome of carotid IPH with carotid imaging predictors including percent diameter stenosis, mm stenosis, maximum plaque thickness, ulceration, and intraluminal thrombus. Clinical covariates included age, male sex, diabetes, hypertension, hyperlipidemia and body mass index. Cardiovascular medication confounders included antihypertension, antiplatelet, anticoagulation and statin medication classes. In addition, magnet strength (3T or 1.5T) was included as a potential confounder in the logistic regression model. A backwards-elimination method was used to determine the final model, in which all remaining predictors had a $p<.10$. Odds ratios and p values were reported for each factor alone and for the factors found to be significant from the backward elimination. Receiver operating characteristic (ROC) comparison analysis was performed to determine the discriminatory value of the final model compared to (1) a model using only plaque thickness, (2) a model using only percent stenosis as a continuous variable and (3) a model using only plaque ulceration. All statistical analyses were performed with Stata version 13.1.

Results

Patient Demographics

Patient demographics are listed by vessel and depicted in Table 1.

Carotid plaque markers and stroke imaging

The carotid imaging features used in this study included the outcome, IPH, and predictors including percent diameter stenosis, mm stenosis, maximum plaque thickness, ulceration, and intraluminal thrombus as described in the methods (Figure 1).

Multivariable logistic regression

Intraplaque hemorrhage predictors are depicted in Table 2, with odds ratios adjusted using multivariable logistic regression.

Final multivariable logistic regression model

The final model for predictors of carotid IPH is depicted in Table 3. After backward-elimination with a threshold of p<.10, the remaining significant factors predicting carotid IPH included maximum plaque thickness (OR=2.20, p<.001, 95% confidence interval (CI) = 1.50, 3.22), mm stenosis (OR=0.46, p<.001, 95% CI = 0.30, 0.71), ulceration (OR=4.25, p=.020, 95% CI=1.25, 14.4), age (OR=1.11, p =.001, 95% CI =1.05, 1.18) and male sex (OR=3.23, p=.077, 95% CI = 0.88, 11.9). Please note that mm stenosis is a measure of the lumen diameter (b) at the level of stenosis described in the methods. Thus, carotid plaque with severe stenosis (small b) is associated with IPH, and carotid plaque without stenosis (large b) is not associated with IPH. This accounts for the seemingly counterintuitive OR of 0.46 in the final model. Also, percent diameter stenosis measured by NASCET is not in the final model due to the nonsignificant p>.10 during backwards elimination. If alternatively mm stenosis was not measured, then percent stenosis would meet the p<.10 criteria (Full model: OR=23.7, p=.003, 95%CI = 3.00, 187.2 ; Final model: OR=31.0, p=.001, 95% CI = 3.89, 246.2). However, because we measured both percent and mm stenosis, and mm stenosis was a better predictor of IPH, we have kept it in the final model.

ROC comparison analysis

ROC comparison analysis is shown in Figure 2. The final model discriminatory value was excellent (Area under the curve AUC=0.932), and was significantly higher than models using only plaque thickness (AUC=0.881), only mm stenosis (AUC=0.830) or only ulceration (AUC=0.715), p<.001.

Discussion

Along with other clinical and imaging factors, carotid IPH allows optimal prediction of carotid-sources of stroke.[8] Currently, optimal medical treatment for carotid IPH is unknown. It is therefore essential to determine predictors of IPH. These predictors could be used as surrogate markers to calculate the likelihood for IPH when MRI is not available or is contraindicated. In addition, these predisposing factors may serve as clues to the pathogenesis of IPH.

Lumen imaging is far more often used in the workup of carotid source stroke. CTA is also used more frequently than MRA, by as much as 4 times at our institutions. Lumen imaging of stenosis alone provides poor prediction of IPH.[21] This study demonstrates that the presence of lumen markers such as maximum plaque thickness, mm stenosis, and ulceration combined with the patient's age and whether the patient is male, predict carotid IPH with high discriminatory power.

These results indicate that plaque ulceration is strongly predictive of IPH. This may be because both ulceration and IPH are markers of unstable plaque and frequently coexist. Alternatively, IPH may predispose to endothelial dysfunction, erosion and eventual ulceration through proinflammatory effects of iron on reactive oxygen species formation.[22] Plaque ulceration has been previously suggested as a surrogate marker of carotid IPH.[12] Our research argues that while ulceration is an essential predictor of IPH, it cannot fully act as a surrogate for IPH without determining the other clinical and imaging factors in the regression analysis. In the assessment of carotid stroke risk, the presence of ulceration alone could prompt further evaluation with MRI to assess for IPH.

Our study also shows that maximum plaque thickness is an essential predictor of IPH. This suggests that larger plaques are inherently more unstable and prone to hemorrhage, potentially due to a larger lipid rich core, and/or a higher number or more permeable plaque neovessels. Delayed contrast imaging may allow better detection of lipid rich cores and dynamic contrast enhanced-MRI (DCE-MRI) may better characterize microvascularity predisposing to IPH.[23, 24]

In addition to plaque thickness, mm stenosis was a significant indicator of IPH. Interestingly, mm stenosis was a better predictor than percent diameter stenosis, and when both are used % stenosis is eliminated from the final model due to its failure to achieve significance. In support of this, mm stenosis has been shown to be a reliable measurement with low interobserver variability.[19] The single measurement of mm stenosis is without the inherent variability of NASCET ratios with two measurements and variable distal ICA caliber within and between patients.

It is unclear why mm stenosis adds further value to plaque thickness in the prediction of IPH. One possibility is that higher degrees of stenosis are associated with further impaired flow dynamics and oscillatory shear stress. In $ApoE^{-/-}$ mice on a Western diet and treated with angiotensin II and carotid ligation, IPH develops in areas of stenosis and low wall shear stress.[25] This is likely related to altered endothelial cell mechanotransduction, as low mean shear stress and oscillatory shear stress lead to endothelial reactive oxygen species formation in cell culture models.[26–29] The shear stress environment at branch points and stenotic vessels could act to sustain IPH through oxidative stress, chronic plaque inflammation and sustained neovessel permeability.

Of the clinical factors assessed in this study, only patient age and male sex were found to significantly increase the risk of IPH. Both of these factors have been associated with IPH in recent research.[13] Atherosclerosis has long been known to be an age-related phenomenon. Arterial plaques form preferentially at branch points and may be fundamental to the process

of aging, having been found in ancient mummies from at least 4 different cultures.[30] Aging may lead to atherosclerosis via increased levels of oxidative stress, DNA damage, mitochondrial dysfunction, and altered balance of cell proliferation and apoptosis.[31]

While the correlation with age is not surprising, it remains to be seen what specific role male sex plays in the development of IPH. It has long been known that atherosclerosis incidence is lower in women compared to men, but this increases after menopause suggesting an atheroprotective effect of estrogen.[32] However, randomized controlled clinical trials have found no benefit to estrogen therapy in cardiovascular disease.[33] Androgens may also provide benefit to male patients through direct action on the vasculature or through a more favorable lipid profile, though the effect of androgen therapy after andropause is unknown.[34] There may also be sex differences accounting for platelet activation, coagulation and endothelial cell function that may contribute to plaque inflammation and IPH.[35]

In conclusion, this study identifies lumen markers and clinical factors that can predict IPH with a high discriminatory power. These predictors provide clues to the pathogenesis of IPH. Also, when MRI is not available or contraindicated, these markers may allow clinicians to estimate the likelihood of IPH being present. Identifying patients that are likely to be negative for IPH can prevent unneeded surgeries or interventions. Further, pre-screening patients prior to undergoing MRA can significantly improve the positive or negative predictive value of T1-weighted sequences in identifying IPH. This will be important in recruiting patients for future studies aimed at determining optimal IPH treatment.

Conclusions

Optimal prediction of carotid IPH is achieved using information on maximum plaque thickness, mm stenosis, ulceration, patient age, and male sex. These factors can be used to determine IPH with a high discriminatory power and may provide clues to the pathogenesis of IPH. Together, they may also be used to determine if IPH is present in patients in whom MRI is contraindicated.

Acknowledgements

None

Grant support: This investigation was supported by the University of Utah Study Design and Biostatistics Center, with funding in part from the National Center for Research Resources and the National Center for Advancing Translational Sciences, National Institutes of Health, through Grant 8UL1TR000105 (formerly UL1RR025764).

Abbreviation Key

IPH	Intraplaque hemorrhage
MPRAGE	Magnetization-prepared rapid acquisition gradient echo
ROC	Receiver operating characteristic
AUC	Area under the curve

References

1. North American Symptomatic Carotid Endarterectomy Trial C. Beneficial effect of carotid endarterectomy in symptomatic patients with high-grade carotid stenosis. The New England journal of medicine. 1991; 325:445–453. [PubMed: 1852179]
2. Endarterectomy for asymptomatic carotid artery stenosis. Executive Committee for the Asymptomatic Carotid Atherosclerosis Study. JAMA. 1995; 273:1421–1428. [PubMed: 7723155]
3. Randomised trial of endarterectomy for recently symptomatic carotid stenosis: final results of the MRC European Carotid Surgery Trial (ECST). Lancet. 1998; 351:1379–1387. [PubMed: 9593407]
4. Moody AR, Murphy RE, Morgan PS, et al. Characterization of complicated carotid plaque with magnetic resonance direct thrombus imaging in patients with cerebral ischemia. Circulation. 2003; 107:3047–3052. [PubMed: 12796133]
5. Ota H, Yarnykh VL, Ferguson MS, et al. Carotid intraplaque hemorrhage imaging at 3.0-T MR imaging: comparison of the diagnostic performance of three T1-weighted sequences. Radiology. 2010; 254:551–563. [PubMed: 20093526]
6. Yamada N, Higashi M, Otsubo R, et al. Association between signal hyperintensity on T1-weighted MR imaging of carotid plaques and ipsilateral ischemic events. AJNR American journal of neuroradiology. 2007; 28:287–292. [PubMed: 17296997]
7. Takaya N, Yuan C, Chu B, et al. Association between carotid plaque characteristics and subsequent ischemic cerebrovascular events: a prospective assessment with MRI--initial results. Stroke; a journal of cerebral circulation. 2006; 37:818–823.
8. McNally JS, McLaughlin MS, Hinckley PJ, et al. Intraluminal Thrombus, Intraplaque Hemorrhage, Plaque Thickness, and Current Smoking Optimally Predict Carotid Stroke. Stroke; a journal of cerebral circulation. 2014
9. McNally JS, Kim SE, Yoon HC, et al. Carotid magnetization-prepared rapid acquisition with gradient-echo signal is associated with acute territorial cerebral ischemic events detected by diffusion-weighted MRI. Circ Cardiovasc Imaging. 2012; 5:376–382. [PubMed: 22495769]
10. Sun J, Song Y, Chen H, et al. Adventitial perfusion and intraplaque hemorrhage: a dynamic contrast-enhanced MRI study in the carotid artery. Stroke; a journal of cerebral circulation. 2013; 44:1031–1036.
11. Zhao X, Underhill HR, Zhao Q, et al. Discriminating carotid atherosclerotic lesion severity by luminal stenosis and plaque burden: a comparison utilizing high-resolution magnetic resonance imaging at 3.0 Tesla. Stroke; a journal of cerebral circulation. 2011; 42:347–353.
12. U-King-Im JM, Fox AJ, Aviv RI, et al. Characterization of carotid plaque hemorrhage: a CT angiography and MR intraplaque hemorrhage study. Stroke; a journal of cerebral circulation. 2010; 41:1623–1629.
13. Zhao XQ, Hatsukami TS, Hippe DS, et al. Clinical factors associated with high-risk carotid plaque features as assessed by magnetic resonance imaging in patients with established vascular disease (from the AIM-HIGH Study). The American journal of cardiology. 2014; 114:1412–1419. [PubMed: 25245415]
14. Zhu DC, Ferguson MS, DeMarco JK. An optimized 3D inversion recovery prepared fast spoiled gradient recalled sequence for carotid plaque hemorrhage imaging at 3.0 T. Magn Reson Imaging. 2008; 26:1360–1366. [PubMed: 18583079]
15. Hadley JR, Roberts JA, Goodrich KC, et al. Relative RF coil performance in carotid imaging. Magn Reson Imaging. 2005; 23:629–639. [PubMed: 16051037]
16. North American Symptomatic Carotid Endarterectomy Trial. Methods, patient characteristics, and progress. Stroke; a journal of cerebral circulation. 1991; 22:711–720.
17. Fox AJ. How to measure carotid stenosis. Radiology. 1993; 186:316–318. [PubMed: 8421726]
18. Fox AJ, Eliasziw M, Rothwell PM, et al. Identification, prognosis, and management of patients with carotid artery near occlusion. AJNR American journal of neuroradiology. 2005; 26:2086–2094. [PubMed: 16155163]
19. Bartlett ES, Walters TD, Symons SP, et al. Quantification of carotid stenosis on CT angiography. AJNR American journal of neuroradiology. 2006; 27:13–19. [PubMed: 16418349]

20. Menon BK, Singh J, Al-Khataami A, et al. The donut sign on CT angiography: an indicator of reversible intraluminal carotid thrombus? Neuroradiology. 2010; 52:1055–1056. [PubMed: 20625710]
21. Anzidei M, Napoli A, Zaccagna F, et al. Diagnostic accuracy of colour Doppler ultrasonography, CT angiography and blood-pool-enhanced MR angiography in assessing carotid stenosis: a comparative study with DSA in 170 patients. Radiol Med. 2012; 117:54–71. [PubMed: 21424318]
22. Buttari B, Profumo E, Businaro R, et al. Oxidized haemoglobin-driven endothelial dysfunction and immune cell activation: novel therapeutic targets for atherosclerosis. Current medicinal chemistry. 2013; 20:4806–4814. [PubMed: 23834168]
23. Kerwin WS, O'Brien KD, Ferguson MS, et al. Inflammation in carotid atherosclerotic plaque: a dynamic contrast-enhanced MR imaging study. Radiology. 2006; 241:459–468. [PubMed: 16966482]
24. Mendes J, Parker DL, McNally S, et al. Three-dimensional dynamic contrast enhanced imaging of the carotid artery with direct arterial input function measurement. Magnetic resonance in medicine : official journal of the Society of Magnetic Resonance in Medicine/Society of Magnetic Resonance in Medicine. 2014; 72:816–822.
25. Cheng C, Tempel D, van Haperen R, et al. Atherosclerotic lesion size and vulnerability are determined by patterns of fluid shear stress. Circulation. 2006; 113:2744–2753. [PubMed: 16754802]
26. McNally JS, Davis ME, Giddens DP, et al. Role of xanthine oxidoreductase and NAD(P)H oxidase in endothelial superoxide production in response to oscillatory shear stress. American journal of physiology Heart and circulatory physiology. 2003; 285:H2290–H2297. [PubMed: 12958034]
27. Davies PF, Polacek DC, Shi C, et al. The convergence of haemodynamics, genomics, and endothelial structure in studies of the focal origin of atherosclerosis. Biorheology. 2002; 39:299–306. [PubMed: 12122245]
28. Pedersen EM, Oyre S, Agerbaek M, et al. Distribution of early atherosclerotic lesions in the human abdominal aorta correlates with wall shear stresses measured in vivo. European journal of vascular and endovascular surgery : the official journal of the European Society for Vascular Surgery. 1999; 18:328–333.
29. Wentzel JJ, Kloet J, Andhyiswara I, et al. Shear-stress and wall-stress regulation of vascular remodeling after balloon angioplasty: effect of matrix metalloproteinase inhibition. Circulation. 2001; 104:91–96. [PubMed: 11435344]
30. Clarke EM, Thompson RC, Allam AH, et al. Is atherosclerosis fundamental to human aging? Lessons from ancient mummies. Journal of cardiology. 2014; 63:329–334. [PubMed: 24582386]
31. Sobenin IA, Zhelankin AV, Sinyov VV, et al. Mitochondrial Aging: Focus on Mitochondrial DNA Damage in Atherosclerosis - A Mini-Review. Gerontology. 2014
32. Akishita M, Yu J. Hormonal effects on blood vessels. Hypertension research : official journal of the Japanese Society of Hypertension. 2012; 35:363–369. [PubMed: 22297478]
33. Howard BV, Rossouw JE. Estrogens and cardiovascular disease risk revisited: the Women's Health Initiative. Current opinion in lipidology. 2013; 24:493–499. [PubMed: 24184944]
34. Traish AM, Kypreos KE. Testosterone and cardiovascular disease: an old idea with modern clinical implications. Atherosclerosis. 2011; 214:244–248. [PubMed: 20869058]
35. Roy-O'Reilly M, McCullough LD. Sex differences in stroke: the contribution of coagulation. Experimental neurology. 2014; 259:16–27. [PubMed: 24560819]

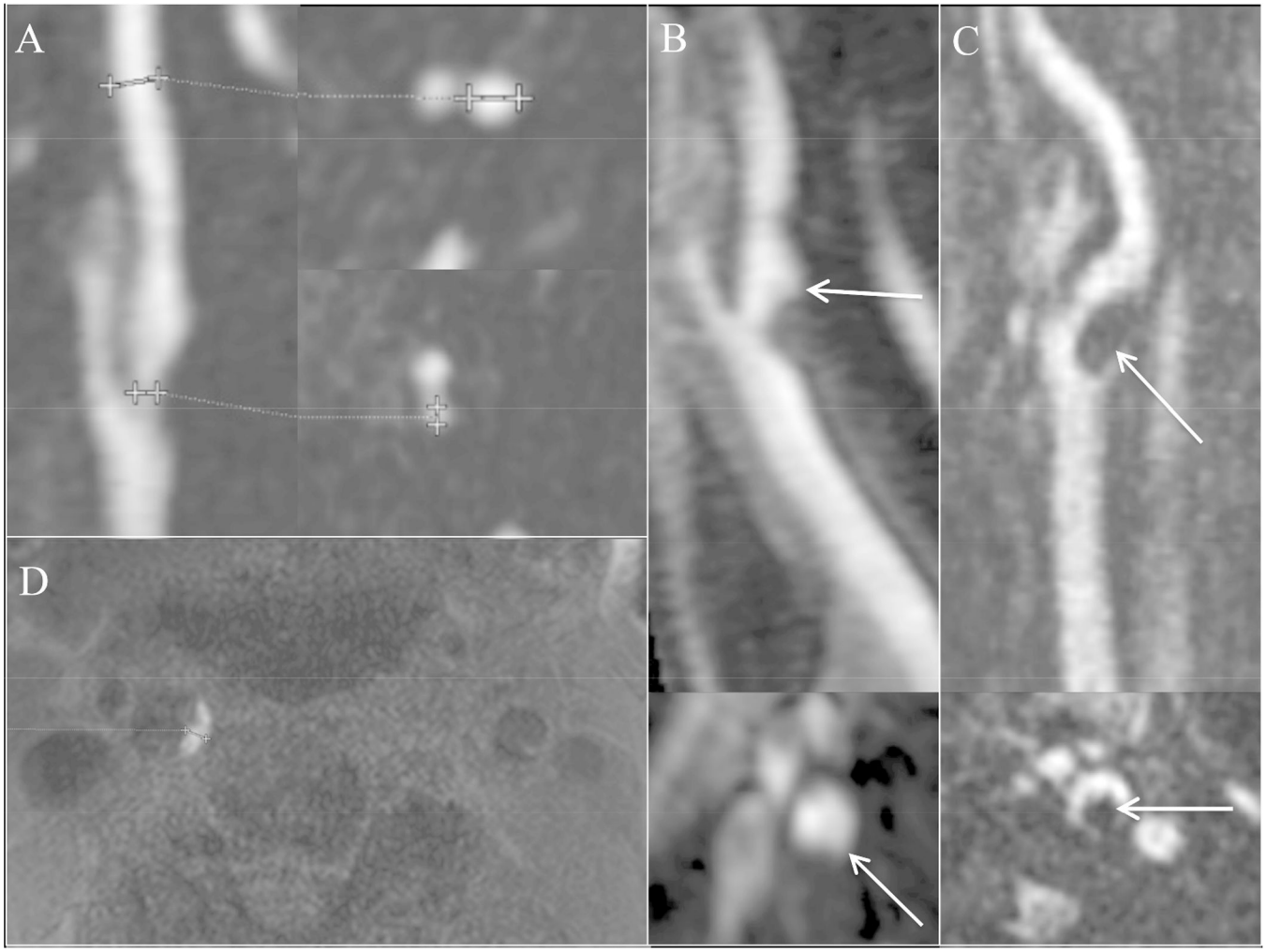

Figure 1.

Carotid plaque imaging markers. Stenosis was measured using percent diameter stenosis [(a −b)/a] and mm stenosis (b) (1A). The presence of ulceration was determined on contrast MRA images using a 2mm measurement threshold (1B). Intraluminal thrombus was defined as a filling defect on contrast MRA images (1C). IPH was defined by MPRAGE-positive plaque, using a signal threshold of 2-fold signal intensity over adjacent sternocleidomastoid muscle (1D, right carotid is MPRAGE-positive, image left). Maximum plaque thickness was measured in the transverse plane on 3D MPRAGE images (1D).

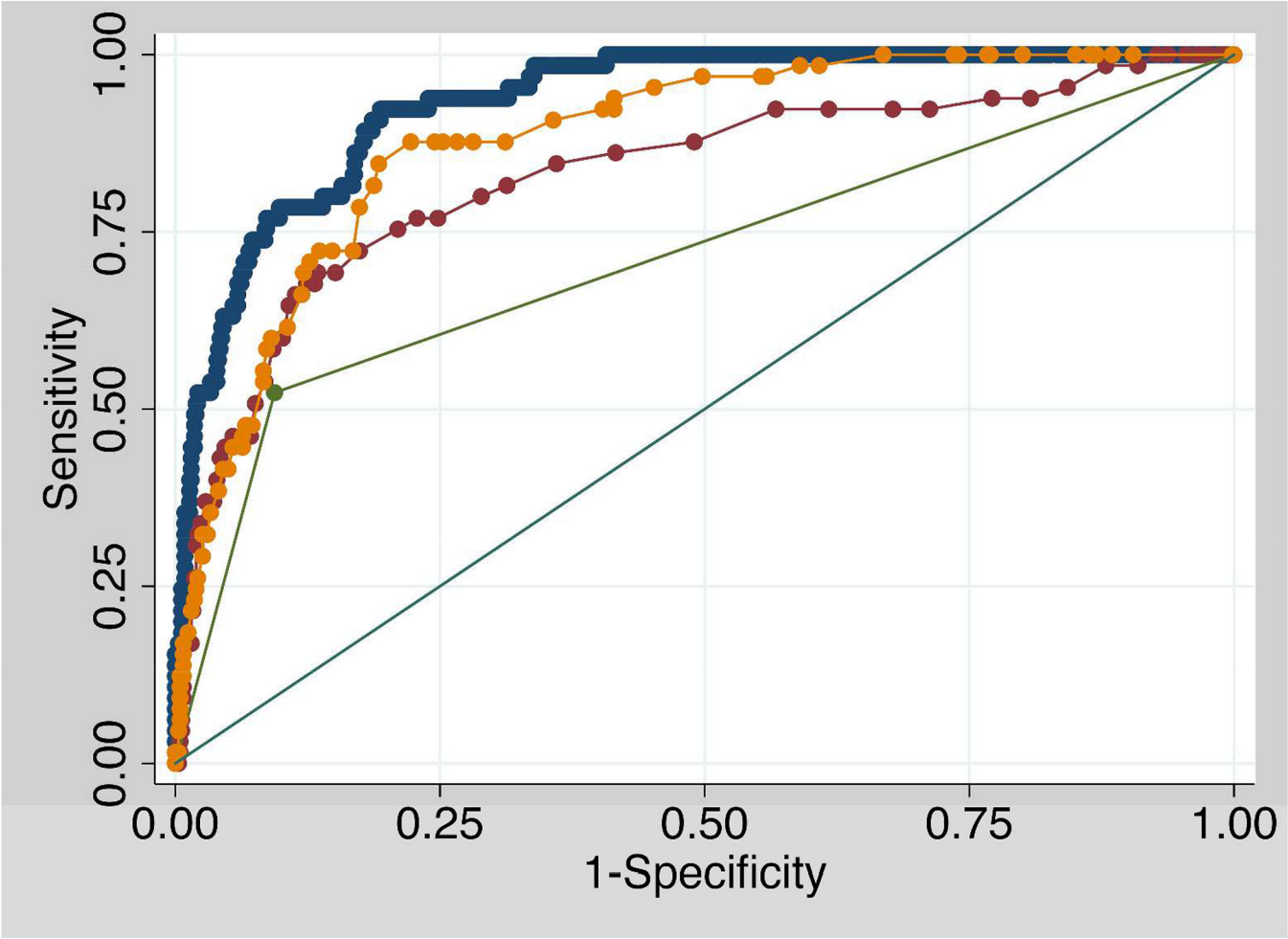

Figure 2.

ROC comparison analysis. The final model IPH discriminatory value was excellent (Blue, AUC=0.932). The final model discriminatory value (Blue) was significantly higher than a model with maximum plaque thickness only (Yellow, AUC=0.881, p<.001), a model with mm stenosis only (Red, AUC=0.830, p<.001), and a model with ulceration only (Green, AUC=0.715, p<.001).

Table 1

Patient demographics

Carotid-stroke predictor	Demographics by vessel
Male sex, no./total no. (%)	387/726 (53.3)
Age, mean (SD), y	64.2 (15.6)
Body mass index (BMI), mean (SD), kg/m^2	28.4 (6.4)
Smoking, no./total no. (%)	
Current smoker	138/726 (19.0)
Prior smoker	158/726 (21.8)
Never smoker	430/726 (59.2)
Hypertension, no./total no. (%)	499/726 (68.7)
Hyperlipidemia, no./total no. (%)	358/726 (49.3)
Diabetes, no./total no. (%)	227/726 (31.3)
Cardiovascular medications	
Antihypertension, no./total no. (%)	412/726 (56.8)
Statin, no./total no. (%)	316/726 (43.5)
Antiplatelet, no./total no. (%)	294/726 (40.5)
Anticoagulation, no./total no. (%)	74/726 (10.2)
Carotid plaque imaging markers	
Stenosis, mean (SD), %	12.2 (23.1)
Mild stenosis (0–49%), no./total no. (%)	647/726 (89.1)
Moderate stenosis (50–69%), no./total no. (%)	45/726 (6.2)
Severe stenosis (70–99%), no./total no. (%)	34/726 (4.7)
Stenosis, mean (SD), mm	4.1 (1.2)
Maximum plaque thickness, mean (SD), mm	3.0 (1.6)
Ulceration, no./total no. (%)	96/726 (13.2)
Intraluminal thrombus, no./total no. (%)	19/726 (2.6)
Intraplaque hemorrhage, no./total no. (%)	65/726 (9.0)
Magnet strength = 3T, no./total no. (%)	58/726 (8.0)

Table 2

Multivariable logistic regression

Carotid-IPH predictor	IPH+ (65)	IPH− (661)	OR	p value	95% CI	
Cardiovascular risk factors						
Male sex, no./total no. (%)	55/65 (70.0)	332/661 (50.2)	3.05	0.104	0.79	11.7
Age, mean (SD), y	76.0 (9.7)	63.1 (15.6)	1.11	0.003	1.04	1.19
BMI, mean (SD), kg/m^2	26.8 (4.0)	28.5 (6.6)	0.94	0.325	0.84	1.06
Smoking, no./total no. (%)						
Current smoker	12/65 (18.5)	126/661 (19.1)	1.52	0.620	0.29	7.88
Prior smoker	24/65 (36.9)	134/661 (20.3)	1.74	0.399	0.48	6.36
Hypertension, no./total no. (%)	46/65 (70.8)	453/661 (68.5)	0.30	0.126	0.06	1.41
Hyperlipidemia, no./total no. (%)	46/65 (70.8)	312/661 (47.2)	1.08	0.895	0.33	3.62
Diabetes, no./total no. (%)	23/65 (35.4)	204/661 (30.9)	1.04	0.948	0.33	3.30
Cardiovascular medications, number/total number (%)						
Antihypertension	43/65 (66.2)	369/661 (55.8)	2.70	0.170	0.65	11.1
Statin	42/65 (64.6)	274/661 (41.5)	1.24	0.749	0.33	4.70
Antiplatelet	38/65 (58.5)	256/661 (38.7)	1.07	0.922	0.29	3.88
Anticoagulation	7/65 (10.8)	67/661 (10.1)	0.63	0.628	0.10	4.00
Carotid plaque imaging markers						
Stenosis, mean (SD), %	46.5 (30.1)	8.9 (19.3)	.09	0.409	0.0003	25.7
Stenosis, mean (SD), mm	2.5 (1.5)	4.3 (1.0)	0.31	0.052	0.09	1.01
Maximum plaque thickness, mean (SD), mm	5.4 (1.9)	2.8 (1.4)	2.26	<0.001	0.09	1.01

Carotid-IPH predictor	IPH+ (65)	IPH− (661)	OR	p value	95% CI	
Ulceration, no./total no. (%)	34/65 (52.3)	62/661 (9.4)	4.36	0.017	1.30	14.7
Intraluminal thrombus, no./total no. (%)	5/65 (7.7)	14/661 (2.1)	0.49	0.496	0.06	3.85
Magnet strength = 3T, no./total no. (%)	16/65 (24.6)	42/661 (6.4)	1.63	0.544	0.34	7.82

Table 3

Final model

Carotid IPH predictor	OR	p value	95% CI	
Ulceration	4.25	0.020	1.25	14.4
Male sex	3.23	0.077	0.88	11.9
Maximum plaque thickness	2.20	<0.001	1.50	3.22
Age	1.11	0.001	1.05	1.18
Stenosis, mm	0.46	<0.001	0.30	0.71